Investigation of giant resonances as doorway states in inelastic nucleon scattering from ^{12}C

H. V. Geramb and K. Amos
Institut für Kernphysik, Kernforschungsanlage, Jülich, West Germany
and School of Physics, University of Melbourne, Parkville, Victoria, Australia, 3052

R. Sprickmann, K. T. Knöpfle,* M. Rogge, D. Ingham,† and C. Mayer-Böricke
Institut für Kernphysik, Kernforschungsanlage, Jülich, West Germany
(Received 24 July 1975)

A formalism for inelastic nucleon scattering from nuclei is developed which takes into account explicitly the effect of giant multipole resonance states. The transition amplitudes derived from this formalism, when energy averaged, separate into two primary components. The first is the slowly energy varying direct reaction amplitude that is mediated by an effective interaction while the second is the energy varying semidirect reaction amplitude associated with doorway state excitations of giant resonances. The determination of quantum numbers and associated properties of giant resonances follow from analyses of inelastic nucleon scattering to low lying nuclear states. Specifically, from the application to the inelastic scattering of 23 to 45 MeV protons from ^{12}C leading to the 1^+ (12.71 MeV $T=0$ and 15.1 MeV $T=1$) states, the strength distributions of the giant isovector $E1$ and isoscalar $E2$ and $E3$ resonances are determined.

[NUCLEAR REACTION $^{12}C(p,p')$, $E=22.5$–45 MeV; measured $\sigma(\theta)$; DWBA analysis; included resonance effects; deduced ^{12}C giant dipole, giant quadrupole strength distribution.]

I. INTRODUCTION

Recently there has been a renaissance in the studies of giant multipole resonances[1-3] due, in large part, to the advent of new experiments. While the isovector giant dipole resonance[4] (GDR) has been extensively studied for at least a decade by means of electromagnetic excitation, it is only in the last few years that other giant multipole resonances have been observed. Prior to this, their existence was inferred by the need of effective charges in shell model calculations[5] of electromagnetic transition rates between low lying states and by the core polarization renormalization in the microscopic description of inelastic nucleon scattering.[6] Now, however, they have been observed directly in photonuclear reactions, particle capture studies,[3] electron[2,8] and hadron scattering,[11-14] and in inelastic scattering to low lying discrete states.[7]

The photonuclear (γ,p) and (γ,n) experiments reveal sensibly only the GDR because of the long range electromagnetic interaction and small momentum transfers involved in those reactions. Inelastic electron scattering to the giant resonance regions permits observation of multipolarities other than the GDR.[2] They are primarily the giant quadrupole[8] (GQR) and giant magnetic dipole[9] (GMD) resonances, for although electron scattering[10] is mediated by the long range electromagnetic interaction, a large range of momentum transfer is involved.

In contrast, direct excitation of giant resonances by hadron scattering does not as clearly display their effects in data since these reactions are mediated by the short ranged nuclear interaction. As a consequence, all transition multipolarities have comparable probabilities. Of course this fact is the great advantage of making studies of giant resonances with hadron scattering experiments since, given the ability to unfold data, information about higher multipole resonances can be obtained. Furthermore, with the variety of projectiles available for nuclear scattering, different giant resonance types can be selectively excited. Specifically, in proton,[11] ^3He,[13] and ^3H scattering all possible electric and magnetic, isoscalar and isovector, excitations are permitted. Deuteron scattering[12] preferentially excites electric and magnetic isoscalar resonances, and α scattering[14] essentially excites only electric isoscalar resonances. However, in all such scattering experiments, the giant resonances are the residual states in the reactions and, since these resonances lie in the continuum, there is considerable difficulty with background subtraction. Thus the resultant data permit neither a sensitive evaluation of the resonance widths nor an estimate of cross section magnitudes to better

than 20%.

Inelastic scattering to low lying states[7] in nuclei is an additional, albeit indirect, way of determining the properties of giant resonances. This occurs when the projectile energy is such that semidirect second order scattering processes mediated by virtual formation of these giant resonances are comparable to those of the normal direct reaction. Then, as the nucleon decay width of giant resonances predominates over any other channel, inelastic nucleon scattering will be most influenced by these semidirect effects. Typically, these giant resonance contributions yield cross sections with magnitudes in the range 0.1 to 1 mb/sr. These are significant contributions in all inelastic channels, the elastic channel included. Hence, as there are a great variety of final states of different spin and parity, and since the inelastic scattering to each of these states will be influenced by semidirect processes, the disadvantage of having to unfold the semidirect and direct contributions is greatly offset by the variety and obtainable accuracy of pertinent data. Of course, to use this method, it is necessary to have full angular distribution inelastic scattering data in small steps of projectile energy, acquisition of which is not difficult if modern data handling facilities are used.

II. THEORY

In this section, a formal theory of direct reaction inelastic nucleon scattering is developed. It is the basis for the identification of different reaction modes and specifically of that in which giant resonances are treated explicitly. This development is presented in Sec. II B after a discussion, in Sec. II A, of our prejudices as to what is the reaction mechanism. Finally, in Sec. II C, we present the approximations necessary to facilitate evaluations.

A. Phenomenological view of the reaction mechanism

Graphical representations of the dominant direct and semidirect processes that influence direct reaction inelastic nucleon scattering are shown in Fig. 1 for single quasiparticle excitations upon the ground state. The notation of Bohr and Mottelson[15] has been supplemented by the use of double arrows to denote particles in the continuum. It should be remembered that the circles denote an explicit two nucleon scattering process and signify that the Pauli exclusion principle should be treated properly.

The direct processes, illustrated in Fig. 1(a), are those mediated by a single effective two-nucleon interaction. This effective interaction is described by a two-nucleon potential with character and parameter values that have been obtained empirically from studies of inelastic scattering to a variety of target states in a variety of nuclei and for many projectile energies.[16] As such, this effective interaction is independent of target states, target mass, and projectile energy. However, while these numerous analyses have resulted in an optimum form,[17] there is ample evidence that this effective interaction is insufficient to explain data quantitatively and additional scattering processes must be introduced. The next simplest modes of scattering processes are those illustrated diagrammatically in Fig. 1(b), namely the semidirect processes that are mediated by two explicit interactions.

The semidirect processes, that still lead to a final nuclear state being a two quasiparticle excitation from the ground state, are obtained by crossing two of the three outgoing lines in the direct process shown in Fig. 1(a). Three forms of semidirect amplitudes result, each of which has distinct dynamical properties. The first of these, the core polarization renormalization amplitude,[6] affects only the bound state details of the scattering. Therefore, it is projectile energy independent and does not selectively affect any specific partial wave in the single particle continuum wave functions. The intermediate pickup model amplitudes are represented by the second of these diagrams, since a two-nucleon cluster propagates between the interactions. Virtual deuteron formation that has been considered in some numerical evaluations[18] provides examples of these amplitudes. While these amplitudes are slightly energy dependent, at least to the extent that stripping and pickup reactions are, and therefore differ in nature from the core polarization renormalization components, they still affect all partial waves. Also, since the cluster is in the continuum, these amplitudes are a primary source of the imaginary part of the complex t matrix recently used to ana-

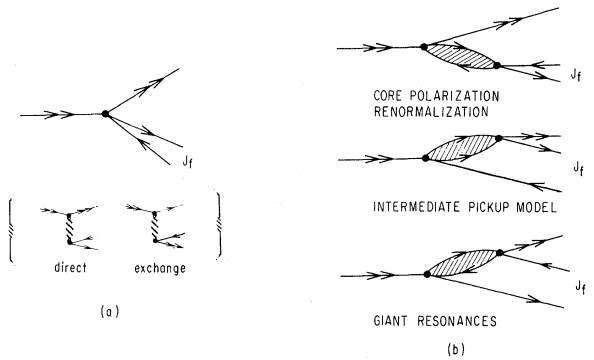

FIG. 1. Diagrammatic representation of the (a) "direct" and (b) semidirect scattering processes for inelastic nucleon scattering to 1p-1h final states in nuclei.

lyze inelastic scattering.[19]

The last of the diagrams in Fig. 1(b) represents resonance processes. They are associated with the excitation of high lying particle-hole states[20] in the target resulting from the capture of the projectile into a bound orbit. The associated scattering amplitudes are significant only if the capture width from the initial channel and the decay width into the final (nucleon emission) channel are large. Such is the case if the intermediate particle-hole states constitute giant resonances which are a group of states within a narrow energy band (< 5 MeV) exhausting a large fraction of the energy weighted sum rule.[21] Therefore, the semidirect resonance scattering amplitudes are significant only for energies spanning these giant resonances. Specifically, using either the collective or naive shell model to predict the giant resonance centroid energies, these semidirect resonance effects will be evident in proton inelastic scattering with projectile energies in the range

$$E_p\,(\mathrm{MeV}) = [41n - (-)^{\Delta T}22]A^{-1/3} + \epsilon_j \pm 5\,, \qquad (1)$$

where $0 < n \leq L$ and $(-1)^n = (-1)^L$ for excitation of isoscalar ($\Delta T = 0$) or isovector ($\Delta T = 1$) giant resonances of multipolarity L. The ϵ_j is the (negative) binding energy of the state into which the projectile is captured. For light nuclei ($A \leq 40$), therefore, resonance effects will influence inelastic proton scattering for projectile energies up to, and possibly greater than, 40 MeV. A lower limit must be set since we require compound reaction contributions to be minor. For heavier nuclei, the $A^{1/3}$ dependence in Eq. (1) lowers the upper limit and, in the lead region, all essential effects are below 20 MeV. As a consequence, indirect assessment of giant resonance properties from semidirect contributions in inelastic scattering to low lying states in very heavy nuclei is less useful because of compound reaction effects. For heavy nuclei, therefore, direct excitation of giant resonances by inelastic hadron scattering might be preferential.

B. Formal derivation of the T matrix

The two potential formula for the T matrix[22] is the basis for all distorted wave approximation calculations. For a Hamiltonian

$$\begin{aligned} H &= H_0 + H_1' + H_2' \\ &= H_1 + H_2' \end{aligned} \qquad (2)$$

the T matrix is

$$T_{\beta\alpha}(H) = T_{\beta\alpha}(H_1) + \langle \psi_1^{(-)}(\beta)\,|\,H_2' + H_2' G^{(+)} H_2'\,|\,\psi_1^{(+)}(\alpha)\rangle\,, \qquad (3)$$

where

$$G^{(+)} = (E - H + i\epsilon)^{-1}$$

is the total Green's function. The matrix elements of the total effective interaction that is based upon the residual interaction H_2', are calculated with eigenfunctions of the truncated Hamiltonian H_1, viz.

$$H_1 \psi_1^{\pm}(\gamma) = E_\gamma \psi_1^{\pm}(\gamma)\,. \qquad (4)$$

To adapt this formulation to calculations, the Hamiltonian H_1 must be specified so that its eigenfunctions can be readily obtained. Whatever be this choice, the difficulties of making calculations are associated with the specifications of the total effective interaction. An input bias as to the important features of this total effective interaction is necessary. In this study, we input the bias discussed above in Sec. II A, and develop the scattering theory in terms of the Feshbach projection formalism.[23]

Hence, we consider the total scattering wave function in the form

$$\Psi = P\Psi + Q\Psi + R\Psi\,, \qquad (5)$$

where the projection operators are such that P projects out the elastic and the specific final inelastic scattering components of the total wave function and R projects out a set of states embedded in the continuum that can be treated as bound doorway states.[24] The operator Q which projects out all other components, and therefore includes all other energetically allowed open reaction channels, then satisfies the completeness relation

$$P + R + Q = 1\,. \qquad (6a)$$

Using the projection operator properties

$$\begin{aligned} &P^2 = P; \quad Q^2 = Q; \quad R^2 = R \\ &PQ = QP = 0, \text{ etc.}, \end{aligned} \qquad (6b)$$

the Schrödinger equation

$$H\Psi = E\Psi \qquad (7)$$

segments, yielding the set of coupled equations

$$\begin{aligned} (E - H_{PP})P\Psi &= H_{PR}R\Psi + H_{PQ}Q\Psi\,, \\ (E - H_{RR})R\Psi &= H_{RP}P\Psi + H_{RQ}Q\Psi\,, \\ (E - H_{QQ})Q\Psi &= H_{QP}P\Psi + H_{QR}R\Psi\,, \end{aligned} \qquad (8)$$

where $H_{PR} = PHR$, etc.

The Q subspace contains all channels that are treated in an average way to facilitate numerical application. Therefore, we introduce the effective energy dependent and non-Hermitian Hamiltonian

$$\mathcal{H}(E) = H + HQ(E - H_{QQ} + i\epsilon)^{-1}QH \qquad (9)$$

which arises from eliminating $Q\Psi$ from the coupled equations. Equations (8) then become

$$[E-\mathcal{H}_{PP}(E)]P\Psi=\mathcal{H}_{PR}(E)R\Psi\,,$$
$$[E-\mathcal{H}_{RR}(E)]R\Psi=\mathcal{H}_{RP}(E)P\Psi\,. \tag{10}$$

Due to the Q subspace effects in $\mathcal{H}$, these equations yield cross sections that fluctuate rapidly with energy. However, since we wish to investigate the direct and semidirect reaction processes, an energy average is needed to eliminate fine structure in the reaction amplitudes. By doing so with a Lorentzian weight function,[24] the appropriate energy averaged coupled equations can be obtained from Eqs. (9) and (10) by replacing E by $E+\frac{1}{2}iI$, whence

$$[E-\mathcal{H}_{PP}(E+\tfrac{1}{2}iI]P\Psi=\mathcal{H}_{PR}(E+\tfrac{1}{2}iI)R\Psi\,,$$
$$[E-\mathcal{H}_{RR}(E+\tfrac{1}{2}iI]R\Psi=\mathcal{H}_{RP}(E+\tfrac{1}{2}iI)P\Psi\,. \tag{11}$$

These are the generalized optical model equations.

The energy averaged T matrix is then obtained by the replacements

$$H_1\rightarrow\mathcal{H}_{PP}(\mathcal{E})\,,$$
$$H_2'\rightarrow\mathcal{H}_{PR}(\mathcal{E})+\mathcal{H}_{RP}(\mathcal{E})+\mathcal{H}_{RR}(\mathcal{E})\,, \tag{12}$$

where $\mathcal{E}=E+\frac{1}{2}iI$, and from Eq. (3)

$$T_{\beta\alpha}=T_{\beta\alpha}[\mathcal{H}_{PP}(\mathcal{E})]+\langle\psi^{(-)}(\beta)\,|\,(\mathcal{H}_{PR}+\mathcal{H}_{RP}+\mathcal{H}_{RR})[1+G^{(+)}(\mathcal{H}_{PR}+\mathcal{H}_{RP}+\mathcal{H}_{RR})]\,|\,\psi^{(+)}(\alpha)\rangle$$
$$=T_{\beta\alpha}(\mathcal{H}_{PP})+\langle\psi^{(-)}(\beta)\,|\,\mathcal{H}_{PR}G^{(+)}\mathcal{H}_{RP}|\,\psi^{(+)}(\alpha)\rangle \tag{13}$$

since both $\psi^{(\pm)}$ belong to the P subspace and are solutions of

$$(\mathcal{H}_{PP}-E)\psi^{(\pm)}=0. \tag{14}$$

The leading terms in Eq. (13) give the scattering amplitudes for the direct processes, classified in Fig. 1(a), as well as the nonresonant (core polarization and intermediate pickup) semidirect processes that were classified in Fig. 1(b). All of these amplitudes involve complex form factors since the Hamiltonian $\mathcal{H}_{PP}(\mathcal{E})$ is non-Hermitian. These amplitudes can be evaluated by using the coupled channels method with complex transition form factors. In the case of weak transitions, it is sufficient to use the distorted wave approximation[25,26] (two channel coupling), whence

$$T_{\beta\alpha}(\mathcal{H}_{PP})\approx\langle\chi_{\beta}^{(-)}\Phi_{J_f}\,|\,\mathcal{H}_{P_\beta P_\alpha}|\,\mathcal{A}(\chi_{\alpha}^{(+)}\Phi_{J_i}\rangle\rangle\,, \tag{15}$$

where $\mathcal{H}_{P_\beta P_\alpha}$ is the complex effective interaction. It is complex because it includes all Q space effects (but no R space effects) that connect the elastic channel, projected by P_α, to the inelastic channel, projected by P_β.

The remaining terms in Eq. (13) yield the scattering amplitudes for the semidirect resonance processes that were characterized in Fig. 1(b). Since the effective interactions $\mathcal{H}_{RP}$ and $\mathcal{H}_{PR}$ couple into and out of R space from P space, respectively, the Green's function is diagonal in R space so that

$$RG^{(+)}R=\{E-\mathcal{H}_{RR}(\mathcal{E})-\mathcal{H}_{RP}(\mathcal{E})[E-\mathcal{H}_{PP}(\mathcal{E})]^{-1}\mathcal{H}_{PR}(\mathcal{E})\}^{-1} \tag{16}$$

is the effective propagator in these amplitudes. As with the leading terms in the T matrix, these semidirect transition components involve form factors that are complex since there are round trip possibilities in which transitions from P to R space proceed via Q space and vice versa. They compete with the direct P to R space transitions.

Formally, the Green's function of Eq. (16) can be evaluated by using a spectral representation. This requires the eigenfunctions of the full non-Hermitian Hamiltonian in $G^{(+)}$ and of its adjoint, and yields[24]

$$RG^{(+)}R=R|\,\psi_R\rangle\mathfrak{D}^{-1}(E)\langle\psi_R^A|R\,, \tag{17}$$

where the energy denominator is

$$\mathfrak{D}^{-1}(E)=(E-E_R-\Delta_R^{\uparrow}+\tfrac{1}{2}i\Gamma_R^{\uparrow}-\Delta_R^{\downarrow}+\tfrac{1}{2}i\Gamma_R^{\downarrow})^{-1}. \tag{18}$$

The level shifts (Δ) and widths (Γ) arising from the coupling of the R into the Q space yield the spreading quantities denoted by ($\downarrow$) while those arising from the coupling of the R into the P space yield the decay quantities that are labeled by ($\uparrow$). Practically, of course, one cannot solve the exact Schrödinger equation which would be required to evaluate these quantities.

C. Practical forms of the resonance T matrix

Using the distorted wave approximation for $\psi^{(-)}(\beta)$ and $\psi^{(+)}(\alpha)$, the resonance transition amplitudes can be expressed as

$$T_{\beta\alpha}^{(2)}=\langle\chi_{\beta}^{(-)}(0')\Phi_{J_f}(A')\,|\,\mathcal{H}_{PR}RG^{(+)}R\mathcal{H}_{RP}\,|\,\chi_{\alpha}^{(+)}(0)\Phi_{J_i}(A)\rangle\,. \tag{19}$$

Then, in accord with our model assumption for the dominant contributing intermediate states of the $A+1$ particle system and assuming that the associated particle-hole excitations result from effective two-nucleon interactions, these amplitudes can be recast as

$$T^{(2)}_{\beta\alpha} \equiv \langle \chi^{(-)}_{\beta}(0') | \langle \Phi_{J_f}(A') | V_{\rm eff}(0'1') | \xi_{2p-1h}(0'A') \rangle \mathfrak{D}^{-1} \langle \xi_{2p-1h}(0,A) | V_{\rm eff}(01) | \chi^{(+)}_{\alpha}(0) \Phi_{J_i}(A) \rangle \tag{20}$$

with

$$\mathfrak{D}^{-1}(E) = (E - E_{2p-1h} + i\tfrac{1}{2}\Gamma)^{-1} . \tag{21}$$

We restrict consideration to excitation of 1p-1h final states since such transitions most stringently select the type of intermediate state structure in which we are interested. Specifically, in the 2p-1h intermediate states, one of these particles will be frozen into the particular particle orbit of the final state. With this restriction, the resonance amplitudes become

$$\begin{aligned} T^{(2)}_{\beta\alpha} &= \langle \chi^{(-)}_{\beta}(0') | \langle [j_{\rm p}(0) \bar{j}^{-1}_{\rm h}(0')]_{J_f} | V_{\rm eff}(0'1') | \{ [\sigma(1')\rho^{-1}(1')]_{\lambda} j_{\rm p}(0) \}_{\mathcal{J}} \rangle \mathfrak{D}^{-1} \langle \{ j_{\rm p}(0) [\sigma(1)\rho^{-1}(1)]_{\lambda} \}_{\mathcal{J}} | V_{\rm eff}(01) | \chi^{(+)}_{\alpha}(0) \rangle \\ &= \sum (-1)^{j_{\rm h}-m'_{\rm h}} \langle j_{\rm p} j_{\rm h} m'_{\rm p} - m'_{\rm h} | J_f M_f \rangle \langle \lambda j_{\rm p} \mu m_{\rm p} | \mathcal{J}\mathfrak{M} \rangle \langle \lambda j_{\rm p} \mu' m'_{\rm p} | \mathcal{J}\mathfrak{M} \rangle \\ &\quad \times \langle \chi^{(-)}_{\beta}(0') | \{ V_{\rm eff}(0'1') | [\sigma(1')\rho^{-1}(1')]_{\lambda\mu'} \} | \bar{j}_{\rm h}(0') \rangle \mathfrak{D}^{-1} \langle j_{\rm p}(0) | \{ [\sigma(1)\rho^{-1}(1)]_{\lambda\mu} | V_{\rm eff}(01) \} | \chi^{(+)}_{\alpha}(0) \rangle , \end{aligned} \tag{22}$$

where now

$$\mathfrak{D}^{-1}(E) = (E - E^{\mathcal{J}}_{2p-1h} + i\tfrac{1}{2}\Gamma_{\mathcal{J}})^{-1} . \tag{23}$$

The evaluation of these amplitudes requires the specific two particle-one hole spectroscopy of the relevant doorway states. Such spectroscopy can be obtained from Tamm-Dancoff approximation (TDA) and random phase approximation (RPA) calculations. To date, however, no such calculations have been reported for the excitation region of interest. Therefore, to facilitate evaluations, it is necessary to further simplify the transition amplitudes of Eqs. (22) and (23). A useful simplification is to take the limit of the spectator concept in which there is no residual particle-phonon interaction, whence all intermediate states $|[(\sigma\rho^{-1})_{\lambda} j]_{\mathcal{J}}\rangle$ for a given λ and j are degenerate. Closure summations on the total intermediate angular momenta $(\mathcal{J}\mathfrak{M})$ are then possible and yield

$$T^{(2)}_{\beta\alpha} = \mathfrak{D}^{-1}(\bar{Q}) \langle \chi^{(-)}_{\beta}(0') | \langle [j_{\rm p}(0) \bar{j}^{-1}_{\rm h}(0')]_{J_f} | \{ V_{\rm eff}(0'1') | [\sigma(i)\rho^{-1}(1')]_{\lambda\mu} \} \{ [\sigma(1)\rho^{-1}(1)]_{\lambda\mu} | V_{\rm eff}(01) \} | \chi^{(+)}_{\alpha}(0) \rangle , \tag{24}$$

where

$$\mathfrak{D}^{-1}(\bar{Q}) = (\bar{Q} - \hbar\omega_{\lambda} + \tfrac{1}{2} i \Gamma_{\lambda})^{-1} \tag{25}$$

and $\bar{Q}$ is $E_{\rm p} - \epsilon_{j_{\rm p}}$, the sum of the projectile kinetic energy and the binding energy of the spectator. Thus, employing the closure approximation has resulted in an effective transition interaction, predicated upon scattering to a particle-hole final state, that is independent of the particle-hole details of that final state.

The effective transition interaction in Eq. (24) is a product of form factors, namely

$$\begin{aligned} V^{(2)}(0',0) &= \mathfrak{D}^{-1}(\bar{Q}) [\vec{f}_{\lambda}(0') \cdot \vec{f}_{\lambda}(0)]_{00} \\ &= \mathfrak{D}^{-1}(\bar{Q}) \{ V_{\rm eff}(0'1') | [\sigma(1')\rho^{-1}(1')]_{\lambda\mu} \} \{ [\sigma(1)\rho^{-1}(1)]_{\lambda\mu} | V_{\rm eff}(01) \} , \end{aligned} \tag{26}$$

where $\{\ \}$ denotes integrations over coordinates 1′ and 1, respectively. These form factors can be reduced by using the standard multipole expansion of a central force

$$\begin{aligned} V_{\rm eff}(01) &= \sum_{LST} 4\pi \omega_{LST}(r_0 r_1) [\vec{Y}_L(0) \cdot \vec{Y}_L(1)] [\vec{O}_S(0) \cdot \vec{O}_S(1)] [\vec{O}_T(0) \cdot \vec{O}_T(1)] \\ &= \sum_{LSTJ} 4\pi \omega_{LST}(r_0 r_1) [\vec{\mathcal{Y}}_{(LS)J} \times \vec{\mathcal{Y}}_{(LS)J}]_{00} [\vec{O}_T(0) \cdot \vec{O}_T(1)] , \end{aligned} \tag{27}$$

and by using RPA type wave functions for the intermediate particle-hole excitations, namely

$$|[\sigma\rho^{-1}]_{\lambda\mu}\rangle = \sum_{\rm ph} (X_{\rm ph} | [j_{\rm p} \bar{j}^{-1}_{\rm h}]_{\lambda\mu} \rangle + Y_{\rm ph} | [j_{\rm h} \bar{j}^{-1}_{\rm p}]_{\lambda\mu} \rangle) . \tag{28}$$

The resulting effective interaction is

$$V^2(0',0)=\sum 16\pi\mathfrak{D}^{-1}(\overline{Q})(-)^{M_T}O_{TM_T}(0')O_{T-M_T}(0)[X_{p'h'}+(-)^{L'+S'+J+j'_p-j'_h}Y_{p'h'}][X_{ph}+(-)^{L+S+J+j_p-j_h}Y_{ph}]$$
$$\times R^{(L'S'T)}_{p'h'}(0')R^{(LST)}_{ph}(0)[\vec{\mathcal{Y}}_{(L'S')J}(0')\cdot\vec{\mathcal{Y}}_{(LS)J}(0)](-)^{S+L+J+l_p+l'_p}(\hat{j}'_p\hat{j}'_h\hat{j}_p\hat{j}_h\hat{l}'_p\hat{l}'_h\hat{l}_p\hat{l}_h\hat{S}'\hat{S})^{1/2}$$
$$\times\langle l'_p l'_h 00\,|\,L'0\rangle\langle l_p l_h 00\,|\,L0\rangle\begin{Bmatrix} l'_p & \frac{1}{2} & j'_p\\ l'_h & \frac{1}{2} & j'_h\\ L' & S' & J\end{Bmatrix}\begin{Bmatrix} l_p & \frac{1}{2} & j_p\\ l_h & \frac{1}{2} & j_h\\ L & S & J\end{Bmatrix}\delta_{J\lambda}\delta_{M_T0}\,, \tag{29}$$

where $\hat{a}$ denotes $2a+1$ and the radial integrals are denoted by R_{ph}. In general, therefore, this effective transition interaction has central, vector, and tensor components. The central and tensor components with $L=J=\lambda$ (and therefore $L'=J=\lambda$) are associated with the excitation of natural parity (electric) resonances, whereas the components with $L\neq J$ (and therefore also $L'\neq J$ but $S=S'=1$) excite unnatural parity (magnetic) resonances. But the direct excitation of λ-multipole giant resonances by inelastic scattering[27] has shown that normal parity states are most readily seen and that their transitions are dominantly $S=0$. Thus we consider only the central non-spin-flip ($S=0$) components of the effective transition interaction of Eq. (29), namely

$$V^{(2)}(0'0)=\sum\mathfrak{D}^{-1}(\overline{Q})8\pi/(2L+1)(-)^{M_T}O_{TM_T}(0')O_{T-M_T}(0)[X_{p'h'}+(-)^{j'_p-j'_h}Y_{p'h'}][X_{ph}+(-)^{j_p-j_h}Y_{ph}]$$
$$\times R^{L(T)}_{p'h'}(0')R^{L(T)}_{ph}(0)[\vec{Y}_L(0')\cdot\vec{Y}_L(0)](-)^{j_p+j'_p}[\hat{j}_p\hat{j}'_p\hat{j}'_h\hat{j}_h]^{1/2}\langle j_p j_h\tfrac{1}{2}-\tfrac{1}{2}\,|\,L0\rangle\langle j'_p j'_h\tfrac{1}{2}-\tfrac{1}{2}\,|\,L0\rangle\,\delta_{L\lambda}\delta_{M_T0}\,, \tag{30}$$

which has the form of a simple multipole expansion with a separable radial form factor

$$V^2(0'0)=-4\pi\sum\mathfrak{D}^{-1}(\overline{Q})g^T_L(0')g^T_L(0)[\vec{Y}_L(0')\cdot\vec{Y}_L(0)](-)^{M_T}O_{TM_T}(0')O_{T-M_T}(0)\delta_{L\lambda}\delta_{M_T0}\,, \tag{31}$$

where

$$g^T_L(0)=[2/(2L+1)]^{1/2}\sum_{ph}[X_{ph}+(-)^{j_p-j_h}Y_{ph}](-)^{j_p}[\hat{j}_p\hat{j}_h]^{1/2}\langle j_p j_h\tfrac{1}{2}-\tfrac{1}{2}\,|\,L0\rangle R^{L(T)}_{ph}(0)\,. \tag{32}$$

Unfortunately, for most nuclei, the wave functions necessary for the evaluation of these microscopic form factors are unavailable. Nevertheless, from the nature of the radial integrals in Eq. (32), these form factors are surface peaked quantities similar to those used in collective model analyses of inelastic scattering.[27] In fact, since the microscopic theory of collective motion[28] relates the phonon creation and annihilation operators to linear combinations of one particle-one hole operators, we can identify the 2p-1h doorway states in Eq. (22) of the microscopic model with a single particle coupled to a collective phonon, namely

$$|\{[\sigma\rho^{-1}]_\lambda j_p(0)\}_s\rangle\Rightarrow|\{|\lambda\rangle_{coll}j_p(0)\}_s\rangle\,, \tag{33}$$

where $|\lambda\rangle_{coll}$ are giant resonance eigenfunctions of the general Bohr collective Hamiltonian that encompasses harmonic surface, spin, and isospin oscillations.[29] With this collective model description, and using the same approximations as in the preceding development, the transition amplitudes of Eq. (24) can be evaluated using the same form for the effective transition interaction as in Eq. (31), but with radial form factors now obtained from the generalized description of the deformed potential model.[30] Specifically these form factors are

$$g^T_L(0)=[4\pi(2L+1)]^{-1/2}\beta^T_L R\left(\frac{\partial U^T(r)}{\partial r}\right), \tag{34}$$

where U^T is the appropriate optical model potential. These form factors thus determine that the effective interaction is

$$V^2(0'0)=\sum y^T_L(\overline{Q})R_0R_{0'}[\vec{Y}_L(0')\cdot\vec{Y}_L(0)]\left(\frac{\partial U^T(r_{0'})}{\partial r_{0'}}\right)$$
$$\times\left(\frac{\partial U^T(r_0)}{\partial r_0}\right)O_{TM_T}(0')O^\dagger_{TM_T}(0)\delta_{L\lambda}\delta_{M_T0}\,, \tag{35}$$

where

$$y^T_L(\overline{Q})=-\mathfrak{D}^{-1}(\overline{Q})(\beta^T_L)^2[2L+1]^{-1}\,, \tag{36}$$

are the energy dependent complex coupling coefficients used previously.[7] These coupling coefficients carry the gross properties (multipolarity, isospin character, total width, and spectral distribution) of the giant resonance doorway states. Specifically, each deformation parameter β^T_L reflects the transition strength for formation, from

the ground state, of an isoscalar ($T=0$) or isovector ($T=1$) giant resonance of multipolarity $L=\lambda$.

The values of these deformation parameters can be constrained by energy weighted sum rules (EWSR).[1,31] In the case of $N=Z$ nuclei, for each excitation with $L>1$, the EWSR is

$$S_{\mathrm{EW}}^{TL}=\frac{\hbar^2}{2m}\,\frac{3A}{4\pi}LR^{2L-2}, \tag{37}$$

to which, using the collective model description, the giant resonance contributes an amount

$$S_{\mathrm{EW}}^{TL}=\hbar\omega_L(\beta_L^T)^2\left(\frac{3A}{4\pi}\right)^2\frac{R^{2L}}{2L+1}. \tag{38}$$

Thus, the maximum deformation parameter value is that for which the giant resonance exhausts 100% of the EWSR, namely

$$\beta_L^T=\left[L(2L+1)\frac{\hbar^2}{2m}\,\frac{4\pi}{3A}\,R^{-2}(\hbar\omega_L)^{-1}\right]^{1/2}$$
$$=\left[87L(2L+1)\,R^{-2}(A\hbar\omega_L)^{-1}\right]^{1/2}. \tag{39}$$

Similar expressions can be obtained for the isovector dipole excitation,[1,31] whence, again for $N=Z$ nuclei,

$$\beta_1^1=\left[1044(1+0.8x)R^{-2}(A\hbar\omega_1)^{-1}\right]^{1/2}. \tag{40}$$

These deformation strengths so extracted from the sum rules provide estimates of the magnitude of the coupling coefficients $y_L^T(\overline{Q})$, but the strength distribution with energy still requires a detailed knowledge of $\mathfrak{D}^{-1}(\overline{Q})$. If any particular giant resonance consisted of just one isolated doorway state (extreme collective model) then the $\mathfrak{D}^{-1}(\overline{Q})$ is known. However, in practice, this is not the case and so the $y_L^T(\overline{Q})$ variation with energy, which can be determined from experiment by a least squares search procedure, must be explained in terms of a more sophisticated theory of the giant resonances.

III. APPLICATIONS

To apply the foregoing theory of inelastic nucleon scattering, measurements were made of proton scattering from ^{12}C in the energy range between 22.5 and 45 MeV. The experiments were performed using the JULIC cyclotron and data obtained in approximately 2 MeV steps for an energy resolution of 100 keV. The relative accuracy of this data was better than 5% and the uncertainty in the absolute normalization is of the order of 10%.

The target was chosen for a number of reasons. For this light nucleus, the discreet states as well as the giant resonances are well separated. In addition, all significant resonance strength is expected to lie in the excitation region from 20 to 45 MeV so that compound effects in the transitions to be studied are negligible. Further, considerable information about this excitation region in ^{12}C has already been obtained from photonuclear,[32] particle capture,[33] electron scattering,[34] and hadron scattering experiments, as well as from several resonance analyses[35] of reactions on ^{12}C. Most important, however, is the existence of discreet states in ^{12}C, the transitions to which are particularly suitable for analyses with this reaction theory.

While the low lying excited states in ^{12}C are well reproduced by shell model calculations, the associated electromagnetic transition strengths are usually grossly underestimated. This is particularly the case for the 2^+ (4.43 MeV) excitation. However, p shell calculations[36] are successful for the isoscalar and isovector 1^+ states that have excitations of 12.71 and 15.11 MeV, respectively. Specifically, they are both dominated by the $(1p_{1/2}\text{-}1p_{3/2}^{-1})$ configuration upon a doubly magic ^{12}C core and therefore their excitations by inelastic proton scattering are favorable for detailed numerical studies based upon the theory already discussed.

Inelastic proton scattering to unnatural parity states has the additional advantage that the direct scattering processes are strongly hindered. Specifically there is no core polarization renormalization since these states exhaust about 90% of the appropriate sum rules[3] and since the transitions are dominated by the spin-flip amplitudes, the associated cross sections are small. Then, since the resonance amplitudes are not hindered by a spin-flip requirement, their effects will be most evident in data.

Of course, for the appropriate projectile energies, all transitions are influenced by these resonance effects and in Sec. III A this is demonstrated for the elastic and quadrupole transitions. The detailed analyses of the 1^+ transitions are presented in the subsequent sections. In Sec. III B, the calculation specifications are given while in Secs. III C and III D, the significance of the extracted resonance coupling strengths is discussed.

A. Evidence of the resonance effects in the elastic and 2^+ (4.43 MeV) excitations in ^{12}C

Because of the limitation of spectroscopy, no detailed calculations of resonance contributions to these transitions have been made. Rather, standard analyses have been made with the optical model and collective coupled channels methods to reveal the discrepancies between the results of such analyses and data. These discrepancies are con-

sistent with additional resonance contributions to the scattering processes.

In Fig. 2, experimental excitation functions[37] for proton elastic scattering from ^{12}C in the range between 20 and 30 MeV and at three scattering angles are compared with the results of a smooth energy varying optical model calculation. The obvious variation of the data about the optical model prediction is not a diffraction effect explicable by a better optical model potential scattering analysis since the variations are too rapid with energy. Thus, there are resonance effects with the strong resonance region of 18 to 24 MeV.

Coupled channels analyses of the angular distributions for the inelastic scattering of 30 to 38 MeV protons exciting the 2^+ (4.43 MeV) state in ^{12}C are compared with the data in Fig. 3. These results illustrate the character of resonance effects in angular distributions. Specifically, resonance contributions are responsible for the back angle peaks in the data. This results since individual resonance cross sections are symmetric about 90° scattering angle, due to parity conservation,[7] whereas the nonresonant direct reaction cross sections are quite forward peaked. Identical effects are observed in other inelastic scattering transitions in ^{12}C that are not reported herein.[38]

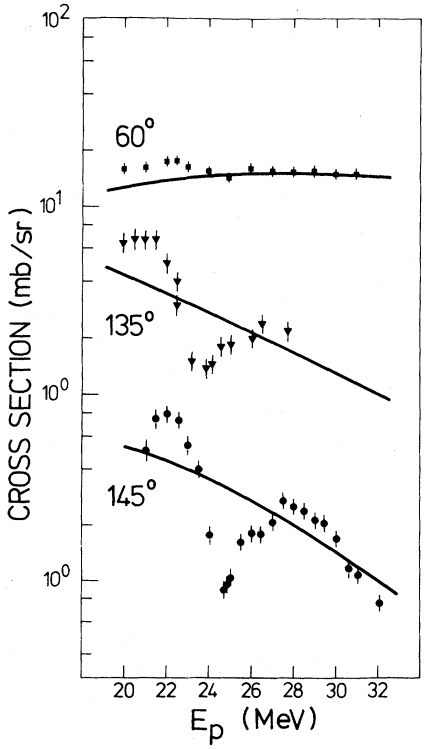

FIG. 2. Excitation functions at the three designated scattering angles for elastic proton scattering from ^{12}C.

B. Specifications of the 1^+ transition calculations

Most details of the calculations for these transitions, namely the spectroscopy of the target states, the parametrization of the effective force, and the procedure by which the complex coupling constants $y_L(\bar{Q})$ of the resonance contributions are extracted have been published[39] and are therefore not repeated. Only the optical model parameters remain to be specified. For proton energies between 20 and 45 MeV, those[40] that gave the smooth results in Fig. 2 were used, while for proton energies below 20 MeV, the optical model parameters were taken from the literature.[41]

Using the least squares fitting procedure[7] to deduce the optimum resonance coupling constants, the resultant fits to data for the isoscalar magnetic dipole transition at 12.71 MeV are shown in Figs. 4(a) and 4(b). The results for the isovector magnetic dipole transition at 15.11 MeV obtained by

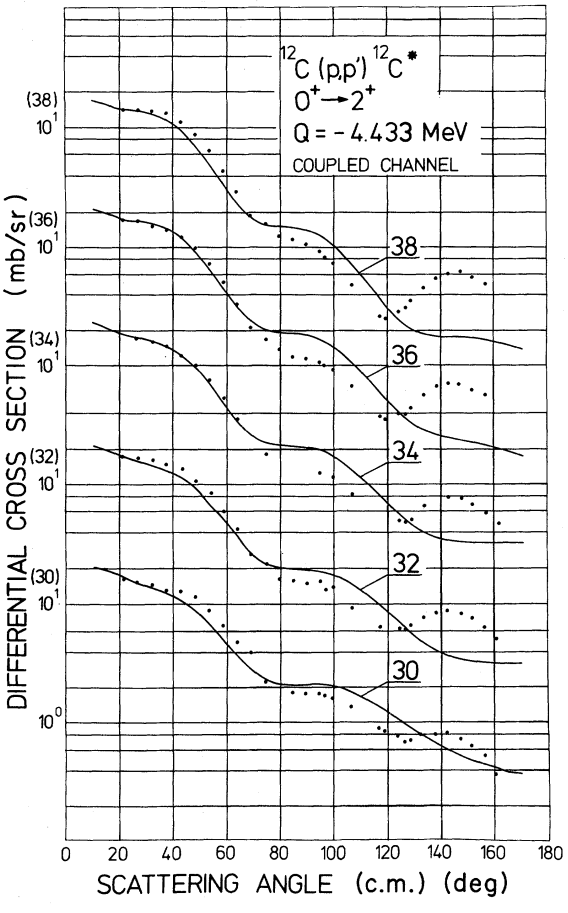

FIG. 3. Coupled channels analyses of proton inelastic scattering to the 2^+ (4.43 MeV) state in ^{12}C for projectile energies between 30 and 38 MeV.

the same procedure are shown in Figs. 5(a) and 5(b).

C. Giant resonance characteristics from the 1^+ transition analyses

The fits to the data shown in Figs. 4 and 5 were obtained by a least squares search for the complex coupling coefficient $y_\lambda(\bar{Q})$ built upon a direct reaction amplitude[26] that was computed with the fixed effective interaction.[39] The magnitudes and phases of the coupling coefficients for $\lambda = 1$, 2, and 3 are shown in Fig. 6 since no other multipolarities, notably those for $\lambda = 0$ and 4, were required in these analyses. It is noteworthy that, by angular momentum selection and independent of model form factors, monopole contributions in these resonance analyses would be isotropic. As such, they are quite distinct from other multipole contributions, in particular from those of the quadrupole resonance. (This technique, therefore, can be used to resolve monopole[42] and quadrupole resonance structure that is inferred by direct excitation to the resonance region by electron and hadron scattering.)

In each distribution, acceptable ranges of coupling coefficient values are given. These ranges result in part from the compromises needed to fit both 1^+ transitions (12.71 and 15.11 MeV excitations) and in part from uncertainties in the resonance form factors due to uncertainties in optical

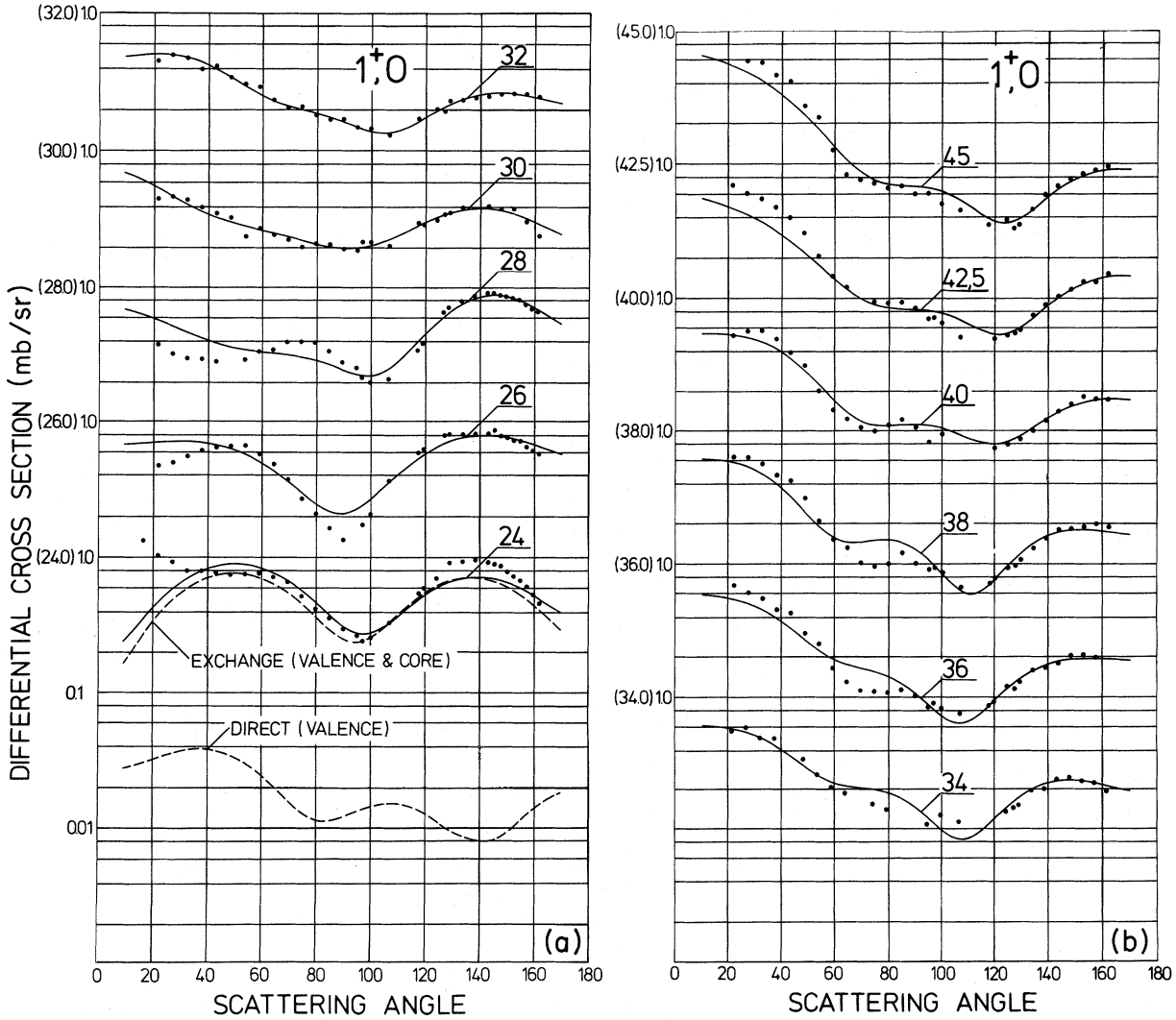

FIG. 4. (a) Differential cross sections for inelastic proton scattering to the 1^+ $T=0$ (12.71 MeV) state in ^{12}C for projectile energies between 24 and 32 MeV. The 24 MeV analysis shows the contributions of the direct processes labeled valence and the semidirect resonance contributions labeled by core. (b) Differential cross sections for inelastic proton scattering to the 1^+ $T=0$ (12.71 MeV) state in ^{12}C for projectile energies between 34 and 45 MeV.

model parameters. This is particularly the case below 26 MeV, and estimates of these uncertainties were obtained by making repeat analyses using different sets of optical model parameters.[41] The ranges of the coupling coefficients below 26 MeV mostly reflect these form factor uncertainties.

It is unfortunate that the large range of tolerable values is associated with the $E1$ excitation since other experimental and theoretical studies[32-34] provide detailed knowledge about this resonance. Despite this variation, the dipole resonance effects dominate analyses of data below 26 MeV sufficiently that gross structure of the resonance can still be ascertained. This is important since it is evidence that the resonances are those of the ^{12}C subsystem in the total compound system of ^{13}N. These distinctions are discussed in the next section.

The tolerable ranges of values of the $E1$ and $E3$ coupling coefficients contain additional correlation effects. These result since the $E3$ contributions influence the same outgoing partial waves as do those of the $E1$. Thus, an increase in $y_1(\overline{Q})$ is somewhat compensated by a decrease in $y_3(\overline{Q})$ and vice versa. While this does not detract from the gross structure we can assign to the $E1$, it does preclude assignation of $E3$ resonance strength.

No such correlations were observed with $y_2(\overline{Q})$, so that information about the quadrupole resonance is most reliable. Specifically, our results show $E2$ resonance strength having an onset at 26 MeV

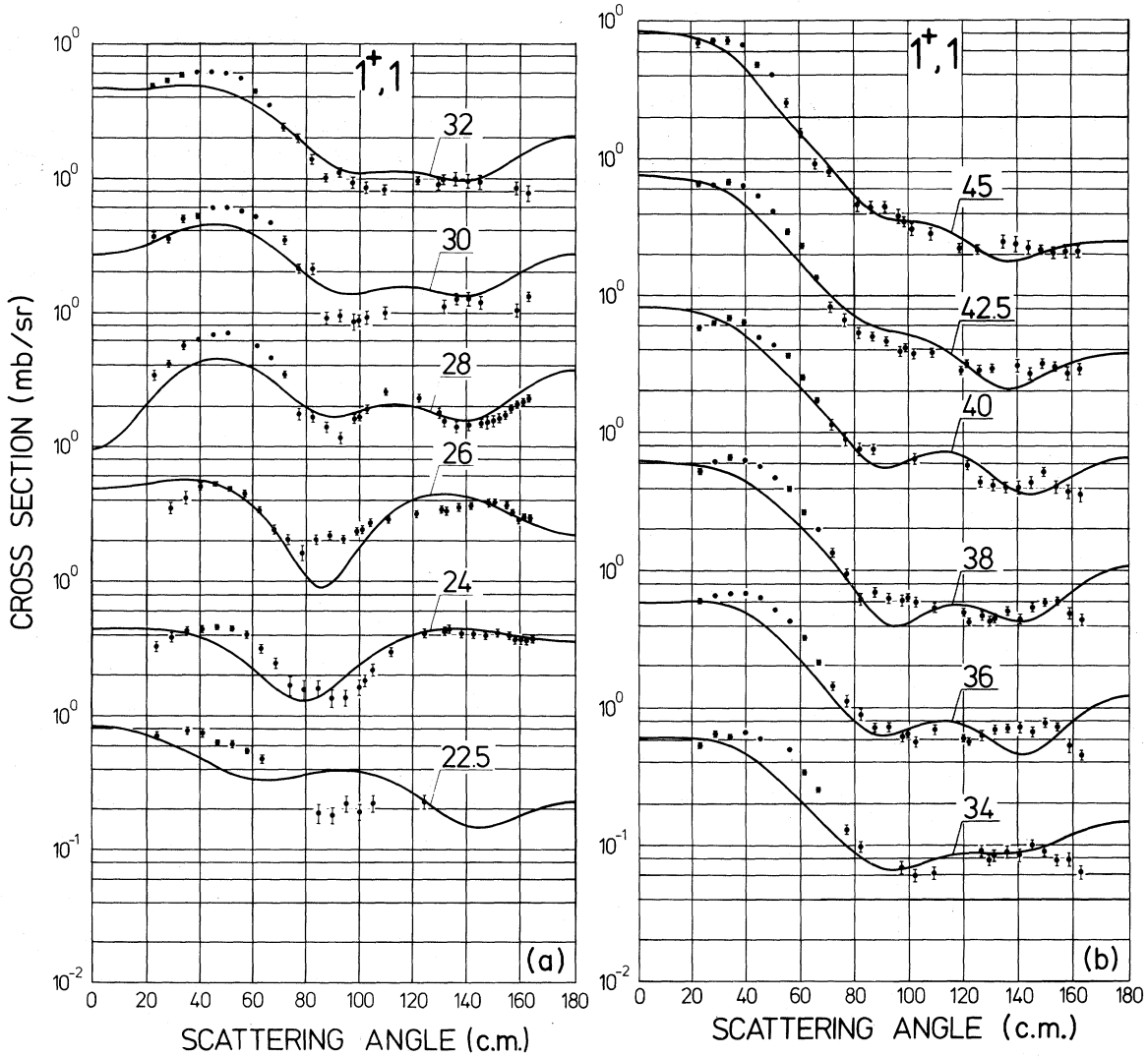

FIG. 5. (a) Differential cross sections for inelastic proton scattering to the 1^+ $T=1$ (15.11 MeV) state in ^{12}C for projectile energies between 22.5 and 32 MeV. (b) Differential cross sections for inelastic proton scattering to the 1^+ $T=1$ (15.11 MeV) state in ^{12}C for projectile energies ranging between 34 and 45 MeV.

with a major peak at 28 MeV and having a gradual decline to the region of 35 MeV. Above this excitation energy, there is weaker evidence of $E2$ strength which one can conjecture to be the isovector resonance. The energy variation of the $y_2(\bar{Q})$, magnitude and phase, is consistent with three $E2$ resonance centroid energies, namely at 28, 32, and 42 MeV, with the widths of the two components at 28 and 32 MeV of this decomposition of the $E2$ resonance distribution being approximately 2 MeV. A binary splitting of this type can be expected from considerations of a naïve shell model since the $E2$ resonance should be dominated by the $2\hbar\omega$ excitations $(1p_{3/2}^{-1}1f_{7/2})$ and $(1p_{3/2}^{-1}1f_{5/2}$ or $2p_{3/2})$. The 28 MeV peak should dominantly contain the $(1p_{3/2}^{-1}1f_{7/2})$ amplitude, and be of isoscalar nature, since with the $y_2(\bar{Q})$ as shown in Fig. 6, $80 \pm 30\%$ of the isoscalar $E2$ EWSR given by Eq. (37) is exhausted by this major peak. It is this comparison (with EWSR) that determines the predominant isospin character of the resonance, since an isovector assignation would overexhaust the appropriate EWSR by several hundred percent.

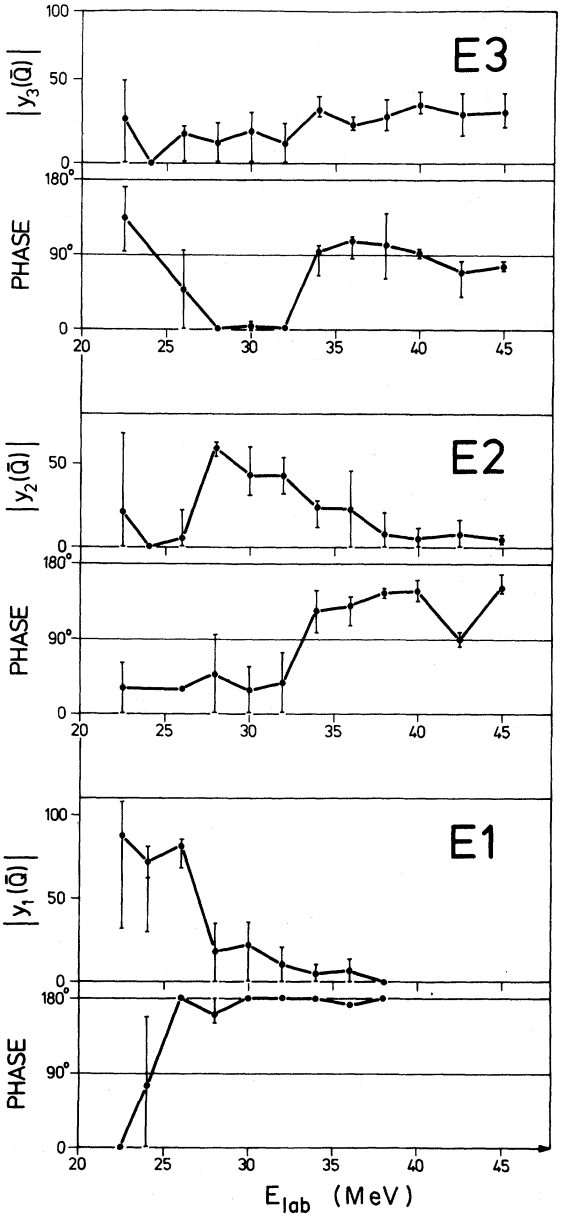

FIG. 6. Strength distributions of the coupling coefficients $y_\lambda(\bar{Q}) = |y_\lambda(\bar{Q})| e^{i\phi_\lambda}$ and $\lambda = 1, 2, 3$, for excitations of the giant dipole, quadrupole, and octupole resonances in an energy range between 22 and 45 MeV.

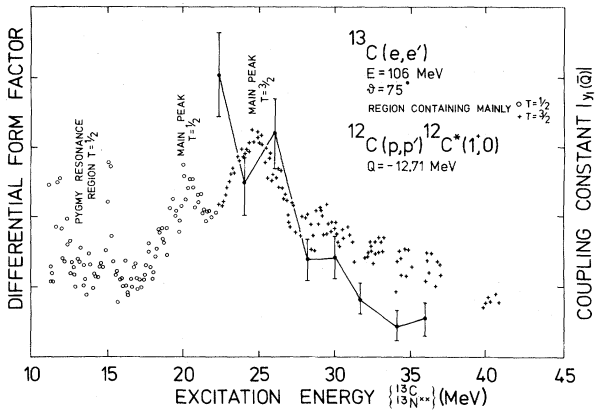

FIG. 7. Giant resonance structure from $^{13}C(e,e')$ compared with the dipole coupling coefficient $|y_1(\bar{Q})|$.

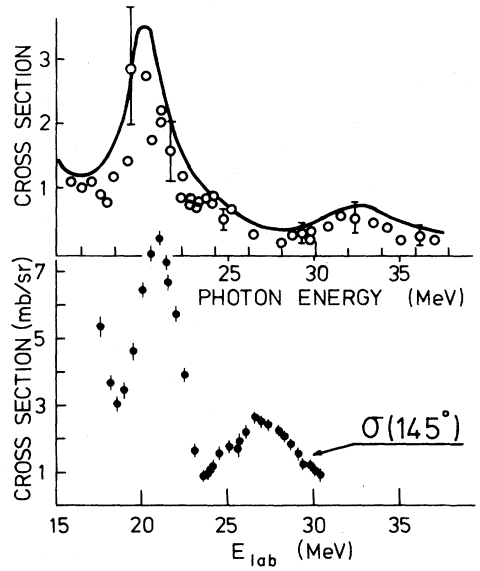

FIG. 8. Comparison of the excitation function for proton elastic scattering from ^{12}C and of the deduced ^{13}N-(γ,p_0) cross section (points) as well as the deduced ^{13}C-(γ,n_0) cross section (curve) as taken from Patrick *et al.* (Ref. 43).

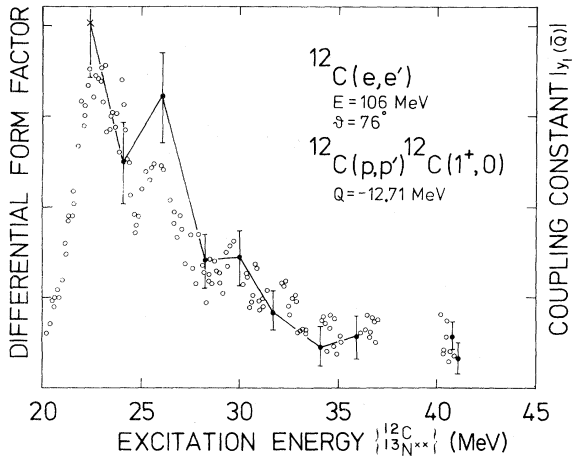

FIG. 9. Comparison of the giant resonance structure from $^{12}C(e,e')$ with the dipole coupling coefficient $|y_1(\bar{Q})|$.

D. Comparison with photonuclear and electron scattering results

In proton scattering from ^{12}C, only the $T=\frac{1}{2}$ fragments of the ^{13}N giant resonances can mediate transitions. This is in contrast to the photonuclear[43] and electron scattering[34] results from the mass 13 system as target in which both the $T=\frac{1}{2}$ and $T=\frac{3}{2}$ components are excited. A typical result for the $E1$ giant resonance as seen by electron scattering on ^{13}C and, assuming charge symmetry, for ^{13}N also, is shown in Fig. 7. From this result, the $E1$ resonance strength is spread in the range from 10 to 35 MeV with considerable fragmentation. The isospins of these fragments have been established by many experimental and theoretical studies and are as identified in Fig. 7. It is to be noted in particular that the $T=\frac{1}{2}$ fragments comprise a pygmy resonance at 13.5 MeV and a main peak at 20 to 21 MeV and with little remaining strength at higher excitations as observed in $^{12}C(p,\gamma)$ studies,[44] while the $T=\frac{3}{2}$ fragments have a single major peak at 25 MeV and further strength at higher excitations. In our analyses of inelastic scattering, the range of excitation energies coincides in the $^{13}N(^{13}C)$ system with the $T=\frac{3}{2}$ fragments. Consequently, our analyses do not reflect the giant resonance structure as observed by $^{13}C(ee')$ and $^{13}C(\gamma,n)$ or, as can be expected, for $^{13}N(\gamma,p)$. Because of this isospin restriction in proton scattering from ^{12}C, the pertinent comparison would therefore be with $^{12}C(p,\gamma_0)$ data. In fact, the comparison of the elastic scattering excitation function and the proton capture cross sections, as shown in Fig. 8, verifies that the $T=\frac{1}{2}$ components of the mass 13 giant resonances influence the elastic scattering. This can be corroborated by the observed abnormalities in the smooth

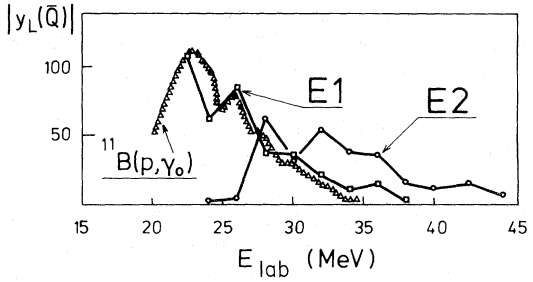

FIG. 10. Comparison of the giant resonance structure from $^{11}B(p,\gamma_0)$ with the dipole and quadrupole coupling coefficients $|\gamma_1(\bar{Q})|$ and $|y_2(\bar{Q})|$.

behavior of the optical model parameters[41] around 14 MeV, where, in ^{13}N, the equivalent of the ^{13}C pygmy resonance is to be expected. However, the gross structure of the $y_1(\bar{Q})$ strength distribution determined from our analyses of the 1^+ transitions is quite different from the $^{12}C(p,\gamma_0)$ results even allowing the large tolerances in each $y_1(\bar{Q})$.

Transitions to the 1^+ states, unlike the elastic scattering, require residual particle-hole excitations and these impose severe restrictions upon the possible set of intermediate states. Specifically, from all possible 2p-1h intermediate states only those in which one particle is in the state $j_p(0)$ ($\equiv 1p_{1/2}$) are permitted. Thus the degrees of freedom of the 13 particle intermediate system are severely restricted to those associated with the 12 nonfrozen particles. Consequently the resonance effects as observed in the 1^+ transitions are to be associated with giant resonances in ^{12}C. Specifically, as revealed by electron scattering from ^{12}C and from proton capture on ^{11}B, the $E1$ resonance strength has its onset at 20 MeV, a major strength concentration around 23 MeV, and a secondary peak around 26 MeV in excitation. These features are shown in Fig. 9 for the electron scattering from ^{12}C and in Fig. 10 for the proton capture by ^{11}B, and are compared with the $y_1(\bar{Q})$ distribution resulting from the 1^+ analyses.

IV. SUMMARY

A direct reaction theory of inelastic scattering has been developed in which giant resonances are treated explicitly as doorway states in the reaction process. Evaluations with this theory were facilitated by imposing approximations, the most significant of which concerns the spectroscopy of the doorway states.

From application to proton scattering exciting the 1^+ states in ^{12}C, the structure of the isovector $E1$ and isoscalar $E2$ resonance distributions in ^{12}C were extracted. The $E1$ distribution confirmed the results of electron scattering and proton capture studies. The $E2$ distribution is predicted to

onset at 26 MeV with a major concentration of strength at 28 MeV and subsidiary strength around 32 and 42 MeV. The latter is conjectured to be part of the isovector quadrupole resonance. Because of this fragmentation of $E2$ strength, it is of great interest to have 1^+ transition data at much smaller energy intervals, so that a more detailed specification of the $E2$ strength distribution can be made. In addition, because of the sensitivity of spin dependent data to these resonance contributions, analyzing power and/or polarization data from these reactions would be most significant.

Two of us (HVG and KAA) wish to express their sincere appreciation for the hospitality, encouragement, and financial assistance provided during their respective noncontemporary leaves of absence at each other's home institutions.

---

*Present address: Max Planck Institut für Kernphysik, Heidelberg, Germany.

†Present address: Centre Européen de Recherches Nucléaires, Geneva, Switzerland.

[1]G. R. Satchler, Phys. Rep. 14C, 99 (1974).

[2]Th. Walcher, in *Proceedings of the International Conference on Nuclear Physics, Munich, 1973,* edited by J. de Boer and H. J. Mang (North-Holland, Amsterdam/American Elsevier, New York, 1973).

[3]S. S. Hanna, in *Proceedings of the International Conference on Nuclear Structure and Spectroscopy, Amsterdam, 1974,* edited by H. P. Blok and A. E. L. Dieperink (Scholar's Press, Amsterdam, 1974).

[4]B. M. Spicer, *Advances in Nuclear Physics,* edited by M. Baranger and E. Vogt (Plenum, New York, 1969), Vol. 2; E. G. Fuller, H. M. Gerstenberg, H. Van der Molen, and T. C. Dunn, U. S. Natl. Bur. Stand. Report No. NBS SP-380, 1973 (unpublished).

[5]A. de-Shalit and H. Feshbach, *Theoretical Nuclear Physics, Vol. 1: Nuclear Structure* (Wiley, New York, 1974).

[6]W. G. Love and G. R. Satchler, Nucl. Phys. A101, 424 (1967); J. Atkinson and V. A. Madsen, Phys. Rev. C 1, 1377 (1970); V. R. Brown and V. A. Madsen, *ibid.* 11, 1298 (1975).

[7]H. V. Geramb, Nucl. Phys. A183, 582 (1972); H. V. Geramb, R. Sprickmann, and G. L. Strobel, Nucl. Phys. A199, 545 (1973); K. A. Amos and R. Smith, *ibid.* A226, 519 (1974).

[8]A. Yamaguchi, T. Terasawa, K. Nakahara, and Y. Torizuka, Phys. Rev. C 3, 1750 (1971); Y. Torizuka *et al.*, in *Proceedings of the International Conference on Nuclear Structure Studies Using Electron Scattering and Photoreactions, Sendai, Japan, 1972,* edited by K. Shoda and H. Ui (Tohoku Univ., Sendai, Japan, 1972); F. R. Buskirk *et al.*, Phys. Lett. 42B, 194 (1972); S. Fukuda and Y. Torizuka, Phys. Rev. Lett. 29, 409 (1972); M. Nagao and Y. Torizuka, *ibid.* 30, 1068 (1973).

[9]R. Pitthan and Th. Walcher, Phys. Lett. 36B, 563 (1971).

[10]H. Überall, *Electron Scattering from Complex Nuclei* (Academic, New York, 1971).

[11]M. B. Lewis and F. E. Bertrand, Nucl. Phys. A196, 337 (1972); M. B. Lewis, F. E. Bertrand, and D. J. Horen, Phys. Rev. C 8, 398 (1973); D. C. Kocher, F. E. Bertrand, E. E. Gross, R. S. Lord, and E. Newman, Phys. Rev. Lett. 31, 1070 (1973); D. J. Horen, F. E. Bertrand, and M. B. Lewis, Phys. Rev. C 9, 1607 (1974); M. B. Lewis and D. J. Horen, *ibid.* 10, 1099 (1974); M. Buenerd, P. de Saintignon, P. Martin, and J. M. Loiseaux, Phys. Rev. Lett. 33, 1233 (1974); N. Marty, M. Morlet, A. Willis, V. Comparat and R. Frascaria, Nucl. Phys. A238, 93 (1975); Orsay Report No. IPNO-PhN-75-11, 1975 (unpublished).

[12]C. C. Chang, F. E. Bertrand, and D. C. Kocher, Phys. Rev. Lett. 34, 221 (1975).

[13]A. Moalem, W. Benenson, and G. M. Crawley, Phys. Rev. Lett. 31, 482 (1973); Nucl. Phys. A236, 307 (1974); R. J. Peterson, *ibid.* A202, 557 (1973).

[14]J. M. Moss, C. M. Rosza, J. D. Bronson, and D. H. Youngblood, Phys. Lett. 53B, 51 (1974); L. L. Rutledge and J. C. Hiebert, Phys. Rev. Lett. 32, 551 (1974); J. M. Moss, C. M. Rosza, D. H. Youngblood, J. D. Bronson, and A. D. Bacher, *ibid.* 34, 748 (1975).

[15]A. Bohr and B. R. Mottelson, *Nuclear Structure* (Benjamin, New York, 1969), Vol. 1.

[16]S. M. Austin, in *The Two-Body Force in Nuclei,* proceedings of a symposium held at Gull Lake, Michigan, 1971, edited by S. M. Austin and G. M. Crawley (Plenum, New York, 1972).

[17]W. G. Love and G. R. Satchler, Nucl. Phys. A159, 1 (1970); L. W. Owen and G. R. Satchler, Phys. Rev. Lett. 25, 1720 (1970); C. W. Wong and C. Y. Wong, Nucl. Phys. A91, 433 (1967).

[18]R. S. Mackintosh, Nucl. Phys. A209, 91 (1973); A230, 195 (1974).

[19]G. R. Satchler, Phys. Lett. 35B, 279 (1971); Z. Phys. 260, 209 (1973); Y. Terrien, Nucl. Phys. A199, 65 (1973); R. M. Halbert and G. R. Satchler, *ibid.* A233, 265 (1974); H. V. Geramb and P. E. Hodgson, *ibid.* A246, 173 (1975).

[20]H. V. Geramb, Nucl. Phys. A183, 582 (1972).

[21]M. B. Lewis, in *Proceedings of the International Conference on Photonuclear Reactions and Applications, Asilomar, 1973,* edited by B. L. Berman (Lawrence Livermore Laboratory, Univ. of California, 1973).

[22]R. Newton, *Scattering Theory of Waves and Particles,* (McGraw-Hill, New York, 1966).

[23]H. Feshbach, Ann. Phys. (N.Y.) 5, 397 (1958); 19, 287 (1962).

[24]H. Feshbach, A. K. Kerman, and R. H. Lemmer, Ann. Phys. (N.Y.) 41, 230 (1967); A. Mekjian, *Advances in Nuclear Physics,* edited by M. Baranger and E. Vogt (Plenum, New York, 1974), Vol. 7; C. Mahaux and H. A. Weidenmüller, *Shell Model Approach to Nuclear Reactions* (North-Holland, Amsterdam, 1969).

[25]N. Austern, *Direct Nuclear Reaction Theories* (Wiley, New York, 1970).

[26]H. V. Geramb and K. A. Amos, Nucl. Phys. A163, 337 (1971).

[27]G. R. Satchler, Nucl. Phys. A195, 1 (1972).

[28]J. M. Eisenberg and W. Greiner, *Nuclear Models* (North-Holland, Amsterdam, 1970).
[29]A. Bohr and B. R. Mottelson, *Nuclear Structure* (Benjamin, New York, 1972), Vol. 2.
[30]C. F. Clement, A. M. Lane, and J. R. Rook, Nucl. Phys. 66, 273 (1965); W. G. Love and G. R. Satchler, Nucl. Phys. A172, 449 (1971).
[31]E. K. Warburton and J. Weneser, *Isospin in Nuclear Physics*, edited by D. H. Wilkinson (North-Holland, Amsterdam, 1969).
[32]B. L. Berman, Univ. of California Radiation Laboratory Report No. UCRL-74622, 1973 (unpublished); E. G. Fuller, H. M. Gerstenberg, H. Van der Molen, and T. C. Dunn, U. S. Natl. Bur. Stand. Report No. NBS SP-380, 1973 (unpublished).
[33]M. Hasinoff, D. Johnson, and D. F. Measday, Phys. Lett. 39B, 506 (1972); C. Brassard, H. D. Shay, J. P. Coffin, W. Scholz, and D. A. Bromley, Phys. Rev. C 6, 53 (1972).
[34]J. C. Bergstrom, H. Crannell, F. J. Kline, J. T. O'Brien, J. W. Lightbody, Jr., and S. P. Fivozinsky, Phys. Rev. C 4, 1514 (1971).
[35]T. Tamura and T. Terasawa, Phys. Lett. 8, 41 (1964); D. K. Scott, P. S. Fisher, and N. S. Chant, Nucl. Phys. A99, 177 (1967).
[36]V. Gillet and N. Vinh Mau, Nucl. Phys. 54, 321 (1964); S. Cohen and D. Kurath, *ibid.* 101, 1 (1967); J. B. McGrory, private communication.
[37]J. K. Dickens, D. A. Haner, and C. N. Waddel, Phys. Rev. 129, 743 (1963); 132, 2159 (1963).
[38]K. T. Knöpfle, D. Ingham, M. Rogge, and C. Mayer-Böricke, Jülich Report, 1973 (unpublished).
[39]K. A. Amos, H. V. Geramb, R. Sprickmann, J. Arvieux, M. Buenerd, and G. Perrin, Phys. Lett. 52B, 138 (1974).
[40]R. Sprickmann, K. T. Knöpfle, D. Ingham, M. Rogge, C. Mayer-Böricke, and H. V. Geramb, Z. Phys. (to be published).
[41]J. S. Nodvik, C. B. Duke, and M. A. Melkanoff, Phys. Rev. 125, 975 (1962); L. Rosen, P. Darriulat, H. Faraggi, and A. Garin, Nucl. Phys. 33, 458 (1962).
[42]N. Marty, M. Morlet, A. Willis, V. Comparat, R. Frascaria, and J. Kallne, Orsay Report No. IPNO-PhN-75-11, 1975 (unpublished).
[43]B. H. Patrick, E. M. Bowey, E. J. Winhold, J. M. Reid, and E. G. Muirhead, Atomic Energy Research Establishment Report No. AERE-R 7882, 1974 (unpublished).
[44]P. S. Fisher, D. F. Measday, F. A. Nikolaev, A. Kalmykov, and A. B. Clegg, Nucl. Phys. 45, 113 (1963).